

SHIRO: Near-Optimal Communication Strategies for Distributed Sparse Matrix Multiplication

Chen Zhuang^{1,2}, Lingqi Zhang², Benjamin Brock³, Du Wu^{1,2},
 Peng Chen², Toshio Endo¹, Satoshi Matsuoka^{1,2}, Mohamed Wahib²

¹Institute of Science Tokyo, Japan, ²RIKEN Center for Computational Science, Japan, ³Intel Corporation, USA
 {chen.zhuang, lingqi.zhang, du.wu, peng.chen, mohamed.attia}@riken.jp,
 brock@cs.berkeley.edu, endo@scrc.iir.isct.ac.jp, matsu@acm.org

Abstract—**Distributed Sparse Matrix-Matrix Multiplication (SpMM)** is a fundamental operation in numerous high-performance computing and deep learning applications. The major performance bottleneck in distributed SpMM lies in the substantial communication overhead, which limits both performance and scalability. In this paper, we identify and analyze sources of inefficient communication in existing distributed SpMM implementations at two levels and address these inefficiencies by proposing: (1) a fine-grained, sparsity-aware communication strategy that reduces communication overhead by exploiting the sparsity pattern of the sparse matrix, and (2) a hierarchical communication strategy that integrates the sparsity-aware strategy with the common two-tier network architectures in GPU-accelerated systems, to reduce redundant communication across slow network links. We implement these optimizations in a comprehensive distributed SpMM framework, **SHIRO**. Extensive evaluations on real-world datasets show that our framework demonstrates strong scalability up to 128 GPUs, achieving geometric mean speedups of 221.5×, 56.0×, 23.4×, and 8.8× over four state-of-the-art baselines (CAGNET, SPA, BCL, and CoLa, respectively) at this scale.

I. INTRODUCTION

Sparse matrix-dense matrix multiplication (SpMM) is a fundamental operation across numerous computational domains. In high-performance computing, SpMM serves as a critical building block for applications including graph algorithms [1], [2] and block iterative solvers [3]–[6]. In deep learning, SpMM has become the core computational kernel in Graph Neural Networks (GNNs), where it implements message-passing operations [7] in widely-used frameworks such as PyTorch Geometric [8] and Deep Graph Library [9]. Beyond these domains, SpMM also plays an important role in recommendation systems [10] and knowledge graph embeddings [11].

Beyond its broad applicability, that motivates extensive single node SpMM optimizations [12]–[16], optimizing distributed SpMM is essential for handling sparse matrices that exceed single-processor memory capacity. For example, finite element simulations routinely generate matrices with millions of degrees of freedom [17], and graph analytics on social networks and web graphs process adjacency matrices containing billions of nodes and edges [18]–[20]. Such scale necessitates efficient distributed SpMM implementations.

Achieving this efficiency, however, is hindered by communication overhead. As input matrices are distributed across processors, each processor must fetch remote matrix blocks during computation [21]–[24]. This bottleneck is particularly

severe in strong-scaling scenarios such as distributed GNN training, where communication consumes up to 83.3% of execution time on 100 Nvidia V100 GPUs [25] and 85.7% on 192 GPUs [2]. This problem intensifies in modern GPU clusters where computational throughput far exceeds inter-node communication bandwidth [2], [25]–[27].

Extensive research has been conducted to reduce communication overhead in distributed SpMM [2], [21], [23], [25]–[30]. Nevertheless, existing methods still suffer from communication inefficiencies at two levels:

(1) Redundancy caused by communication strategies. Existing communication approaches can be broadly categorized into two types: (i) sparsity-oblivious methods [2], [25], [27], [29], [30] transfer entire dense matrix blocks regardless of the actual sparsity patterns, transmitting unnecessary data that introduces significant communication overhead; (ii) sparsity-aware methods [23], [24], [26], [28] attempt to reduce this overhead by transferring data based on the actual demand determined by the sparse matrix patterns. However, these sparsity-aware approaches still suffer from communication redundancy as they only consider partial sparsity information, failing to fully exploit the complete sparsity pattern.

(2) Flat communication over a hierarchical network. Most existing distributed SpMM methods assume uniform communication costs between processes. However, computing clusters, especially those that are GPU-accelerated, exhibit hierarchical networks where bandwidth decreases across levels, causing redundant data transfers when processes within fast-link groups independently fetch identical data through slow inter-group connections. Although recent work [28] partially addresses this inefficiency, it only supports limited communication strategies that only partially reduce the redundancy.

To address these inefficiencies, we propose **SHIRO**, a communication-efficient distributed framework that jointly optimizes sparsity-aware communication strategies and exploits hierarchical network topology to improve the scalability and performance of distributed SpMM. Our main contributions are:

- **Joint row-column sparsity-aware communication strategy.**

We propose a joint sparsity-aware communication strategy that comprehensively exploits complete sparsity patterns to minimize communication redundancy. We characterize the optimal communication volume problem as a mini-

imum weighted covering problem and provide an optimal polynomial-time algorithm based on graph theory.

- **Hierarchical communication strategy.** We present a hierarchical communication strategy that integrates the proposed sparsity-aware strategy with hierarchical network topologies. By exploiting the two-level structure of hierarchical networks, our approach minimizes communication over bandwidth-limited inter-group links. We further design an overlapping scheduling strategy that exploits the complementary nature between row-based and column-based communication to fully utilize the two-level hierarchical networks.
- Comprehensive experimental results on real-world datasets demonstrate that our framework achieves up to 96.3% communication volume reduction and exhibits strong scalability on up to 128 GPUs on a GPU supercomputer, delivering a geometric mean speedup of 221.5 \times , 56.0 \times , 23.4 \times , and 8.8 \times over four state-of-the-art baselines at this scale.

II. BACKGROUND

A. Distributed SpMM

Sparse Matrix-Matrix Multiplication (SpMM) is a fundamental operation where a sparse matrix \mathbf{A} is multiplied by a dense matrix \mathbf{B} to produce a dense result \mathbf{C} : $\mathbf{C} = \mathbf{A}\mathbf{B}$. For large-scale matrices, distributed SpMM addresses memory constraints and improves performance, where matrices \mathbf{A} , \mathbf{B} , and \mathbf{C} are partitioned into multiple blocks and distributed across different processors. Each processor must communicate with others to retrieve the necessary remote matrix blocks for computing its assigned portion of the result matrix. This paper focuses on 1D row-partitioned distributed SpMM, where all matrices are divided into row blocks and distributed across processors, which is widely adopted in practical applications such as Graph Neural Networks (GNNs) due to its simplicity and effectiveness, as well as its compatibility with sparsity-aware methods, which can exploit the skewed nonzero distributions observed in many datasets. Though we focus on 1D row-partitioned partition strategy, our proposed method can also be generalized to different partitioning strategies.

B. 1D Row-partitioned Distributed SpMM

In 1D row-partitioned distributed SpMM, matrices \mathbf{A} , \mathbf{B} , and \mathbf{C} are partitioned along rows into different row blocks and distributed across processes. As illustrated in Fig. 1(a), matrices \mathbf{A} , \mathbf{B} , and \mathbf{C} are partitioned into $\mathbf{A}^{(0,:)}$ and $\mathbf{A}^{(1,:)}$, $\mathbf{B}^{(0,:)}$ and $\mathbf{B}^{(1,:)}$, and $\mathbf{C}^{(0,:)}$ and $\mathbf{C}^{(1,:)}$, which are allocated to processes P_0 and P_1 , respectively. Under this partitioning scheme, process P_0 is responsible for computing $\mathbf{C}^{(0,:)}$ using $\mathbf{A}^{(0,:)}$ and the complete matrix \mathbf{B} , while process P_1 computes $\mathbf{C}^{(1,:)}$ using $\mathbf{A}^{(1,:)}$ and the complete matrix \mathbf{B} .

In 1D row-partitioned SpMM, each process's sparse matrix block can be divided based on data locality. Taking process P_0 as an example (Fig. 1(a)), its sparse matrix $\mathbf{A}^{(0,:)}$ consists of the diagonal block $\mathbf{A}^{(0,0)}$ that requires only local dense matrix $\mathbf{B}^{(0,:)}$, and the off-diagonal block $\mathbf{A}^{(0,1)}$ that requires remote dense matrix $\mathbf{B}^{(1,:)}$ from process P_1 . This locality pattern naturally leads to a four-stage execution: (1) **Local**

TABLE I: List of notations.

Notation	Description
$\mathbf{A}^{(p,:)}$	Row block of matrix \mathbf{A} owned by process p
$\mathbf{B}^{(p,:)}$	Row block of matrix \mathbf{B} owned by process p
$\mathbf{C}^{(p,:)}$	Row block of matrix \mathbf{C} owned by process p
$\mathbf{A}^{(i,j)}$	Sub-block of \mathbf{A} (row block i and column block j)
a_{ij}	The (i,j) -th element of \mathbf{A}
$\mathbf{a}_{i,:}$	The i -th row of \mathbf{A}
$\mathbf{a}_{:,j}$	The j -th column of \mathbf{A}
M	Number of rows in $\mathbf{A}^{(p,:)}$ and $\mathbf{C}^{(p,:)}$
K	Number of columns in $\mathbf{A}^{(p,:)}$ and rows in $\mathbf{B}^{(p,:)}$
N	Number of columns in $\mathbf{B}^{(p,:)}$ and $\mathbf{C}^{(p,:)}$
sz_{dt}	Size of each data element (in bytes)
μ	Size of minimum vertex cover set
$\text{Cols}(\mathbf{A}^{(i,j)})$	Unique column indices of nonzeros in $\mathbf{A}^{(i,j)}$
$\text{Rows}(\mathbf{A}^{(i,j)})$	Unique row indices of nonzeros in $\mathbf{A}^{(i,j)}$

computation, where P_0 computes with $\mathbf{A}^{(0,0)}$ and local $\mathbf{B}^{(0,:)}$; (2) **Communication**, where P_0 retrieves remote $\mathbf{B}^{(1,:)}$ from P_1 ; (3) **Remote computation**, where P_0 computes with $\mathbf{A}^{(0,1)}$ and the received $\mathbf{B}^{(1,:)}$; and (4) **Result aggregation**, where partial results are summed to obtain final $\mathbf{C}^{(0,:)}$. As the system scales to more processors, the *local computation* decreases while *communication* increases (as each processor's local block $\mathbf{B}^{(0,:)}$ shrinks proportionally while the aggregate size of remote blocks $\mathbf{B}^{(1,:)}$, $\mathbf{B}^{(2,:)} \dots \mathbf{B}^{(n,:)}$ grows proportionally with processors), shifting the primary bottleneck to communication.

III. MOTIVATION

This section presents our motivation for reducing communication overhead. We examine why existing approaches fail to minimize this overhead despite various optimization attempts. Our analysis reveals two fundamental issues: current communication strategies transmit redundant data (Sec. III-A), and they ignore the hierarchical structure of modern interconnects (Sec. III-B). We demonstrate that these problems are interdependent—solving one without the other yields limited benefits—thus motivating our unified approach (Sec. III-C).

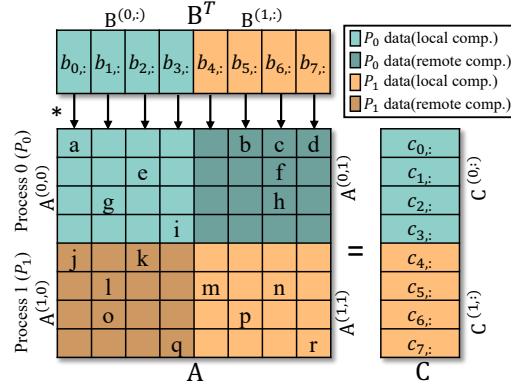
A. Redundancy In Existing Communication Strategies

In 1D row-partitioned distributed SpMM, each process p owns row blocks $\mathbf{A}^{(p,:)}$, $\mathbf{B}^{(p,:)}$, and $\mathbf{C}^{(p,:)}$. To compute its output $\mathbf{C}^{(p,:)}$, each process obtains non-local data by either receiving required rows of \mathbf{B} or collecting partial results of \mathbf{C} from other processes. We examine three representative communication schemes for distributed SpMM, identifying redundancy reduction opportunities. Tab. I summarizes the notations used in our analysis.

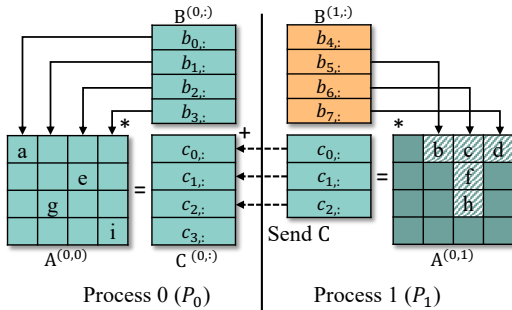
1) **Sparsity-oblivious (block-based) communication:** In the sparsity-oblivious scheme [25], each process fetches complete row blocks $\mathbf{B}^{(i,:)}$ from remote process i , regardless of the sparsity pattern in \mathbf{A} . The communication volume from process i to process j equals the size of row block $\mathbf{B}^{(i,:)}$:

$$V_{\text{block}}^{i,j} = K \cdot N \cdot sz_{dt} \quad (1)$$

2) **Sparsity-aware (column-based) communication:** The sparsity-aware scheme [26], [28] fetches only the rows of \mathbf{B} corresponding to unique column indices of nonzeros in \mathbf{A} . As shown in Fig. 1(b), process P_0 fetches only rows $\mathbf{b}_{5,:}$, $\mathbf{b}_{6,:}$,



(a) 1D partition distributed SpMM. Dark regions: off-diagonal submatrices for SpMM on remote data.



(c) Sparsity-aware (row-based) distributed SpMM from Process 0’s view. P_1 computes partial results and sends required \mathbf{C} rows to P_0 based on unique row indices in $\mathbf{A}^{(0,1)}$. Communication volume is 3 rows.

Fig. 1: Different communication strategies for 1D distributed SpMM.

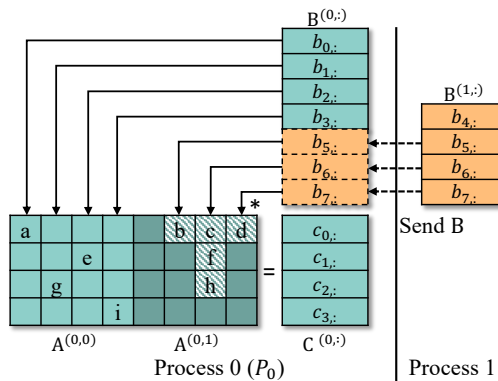
and $\mathbf{b}_{7,:}$ from P_1 based on the nonzero columns in $\mathbf{A}^{(0,1)}$. The communication volume from process i to process j is:

$$V_{\text{col}}^{i,j} = |\text{Cols}(\mathbf{A}^{(j,i)})| \cdot N \cdot sz_{dt} \quad (2)$$

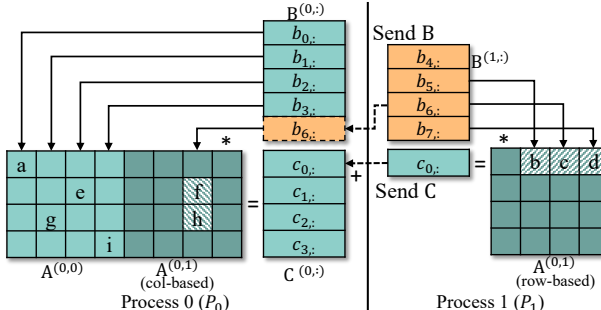
3) Sparsity-aware (row-based) communication: The row-based strategy transfers partial results of \mathbf{C} based on row indices of nonzeros in \mathbf{A} , instead of transferring \mathbf{B} rows based on column indices. As shown in Fig. 1(c), process P_1 computes partial results for rows $\mathbf{c}_{0,:}$, $\mathbf{c}_{1,:}$, and $\mathbf{c}_{2,:}$, corresponding to nonzero rows in $\mathbf{A}^{(0,1)}$ and sends them to P_0 . The communication volume from process i to process j is:

$$V_{\text{row}}^{i,j} = |\text{Rows}(\mathbf{A}^{(j,i)})| \cdot N \cdot sz_{dt} \quad (3)$$

4) Analysis of Communication Redundancy: Existing schemes fail to fully exploit the sparsity structure, leaving significant communication redundancy. The block-based approach ignores sparsity entirely, transferring $K \cdot N$ data regardless of the specific data required by \mathbf{A} ’s sparsity pattern. The sparsity-aware schemes improve upon this by exploiting sparsity in a single dimension—reducing communication to the number of unique columns $|\text{Cols}(\mathbf{A}^{(j,i)})| \cdot N$ (column-based) or the number of unique rows $|\text{Rows}(\mathbf{A}^{(j,i)})| \cdot N$ (row-based). However, as we will demonstrate, single-dimension optimization still leaves substantial redundancy. As illustrated in Fig. 1(d), a joint approach that considers both dimensions can dramatically improve efficiency—for the sparse block $\mathbf{A}^{(0,1)}$, only 2 rows ($\mathbf{b}_{6,:}$ and $\mathbf{c}_{0,:}$) are needed compared to 3



(b) Sparsity-aware (col-based) distributed SpMM from Process 0’s view. P_0 fetches required \mathbf{B} rows from P_1 based on unique column indices in $\mathbf{A}^{(0,1)}$. Communication volume is 3 rows.



(d) Our proposed joint row-column distributed SpMM from Process 0’s view. P_1 computes partial results and sends required \mathbf{B} and \mathbf{C} rows to P_0 . Communication volume reduced from 3 to 2 rows.

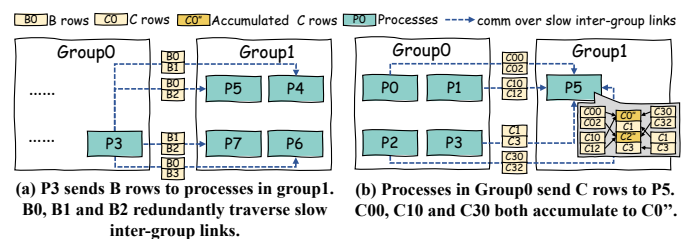


Fig. 2: Redundant data transfers over slow inter-group links. rows for single-dimension approaches. This gap widens for sparser matrices with more complex patterns, motivating a joint optimization framework that simultaneously exploits sparsity in both dimensions.

B. Flat communication over a hierarchical network

In addition to communication redundancy, hierarchical networks introduce another communication inefficiency. Modern GPU-accelerated HPC systems feature multi-level network architectures where intra-group connections significantly outperform inter-group links. For instance [31], GPUs within the same node communicate via NVLink (450GB/s unidirectional link bandwidth on NVIDIA H100 [32]), while cross-node communication relies on InfiniBand HDR (25GB/s [33]), creating an $18\times$ bandwidth disparity. However, standard SpMM implementations use flat all-to-all communication patterns that treat all process pairs equally, ignoring these bandwidth disparities. This topology-oblivious approach creates

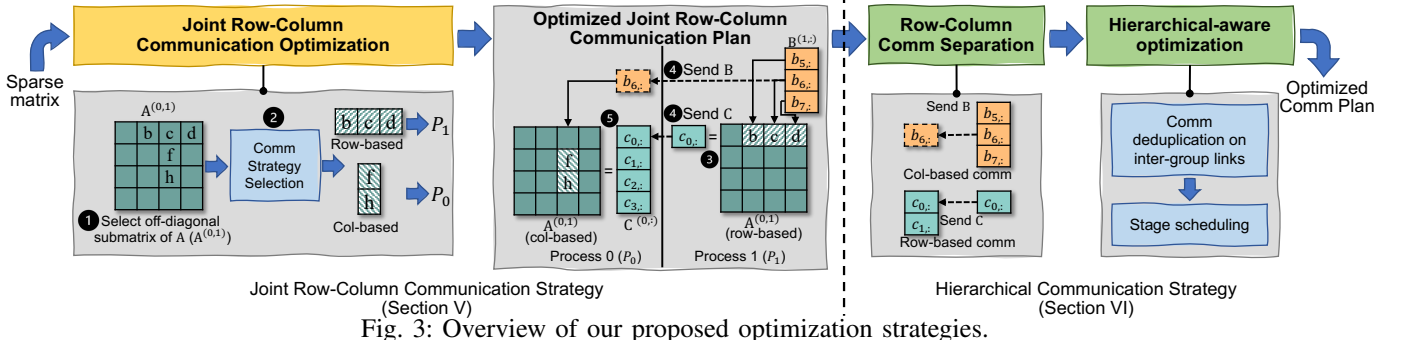


Fig. 3: Overview of our proposed optimization strategies.

redundancy at group boundaries, as illustrated in Fig. 2: (a) identical \mathbf{B} rows (B_0, B_1, B_2) sent to multiple destinations traverse slow inter-group links separately rather than being transmitted once and distributed within the destination group, and (b) partial \mathbf{C} results (C_{00}, C_{10}, C_{30}) targeting the same \mathbf{C} row ($C_{0''}$) cross group boundaries independently instead of being pre-aggregated within the source group. Such hierarchical redundancy significantly increases inter-group traffic, creating bottlenecks as system scale grows.

C. Summary

Optimal performance requires jointly addressing both source of inefficiency that current approaches lacks: communication strategy reduces communication volume but ignores network topology, while hierarchy-aware methods improve bandwidth utilization but retain strategy-level redundancy.

IV. OVERVIEW

We present SHIRO, a unified optimization distributed SpMM framework that jointly addresses communication strategy redundancy and hierarchical network redundancy. SHIRO minimizes total communication volume and inter-group communication through:

- **Joint row-column communication strategy (Sec. V):** Exploits sparsity in row and column dimensions simultaneously, combining row-based and column-based patterns to minimize overall communication volume.
- **Hierarchical communication strategy (Sec. VI):** Adapts this joint row-column communication strategy to the network hierarchy by separating communication into complementary stages and scheduling them to minimize inter-group traffic while maximizing link utilization.

Fig. 3 illustrates the overview of SHIRO’s optimization strategies. Joint row-column optimization analyzes the sparse matrix structure to identify the optimal combination of row-based and column-based strategies, producing a unified communication plan that minimizes total communication volume beyond single-strategy limitations (Sec. V). The hierarchical communication strategy (Sec. VI) then separates the joint communication strategy into independent row-based and column-based communication, enabling each to eliminate inter-group redundancy individually through communication duplication (Sec. VI-A). After independent optimization, these operations are recombined by exploiting their complementary network

link requirements, achieving overlapped execution to maximize link utilization (Sec. VI-B).

V. JOINT ROW-COLUMN COMMUNICATION STRATEGY

This section presents our joint row-column optimization approach that eliminates communication redundancy by optimally assigning each nonzero element in the sparse matrix to use the row-based or column-based strategy. This involves partitioning nonzeros based on either their row or column indices, whichever is communication optimal, then using the respective row- and column-based communication strategies for each set of nonzeros. We first introduce the detailed workflow of our method (Sec. V-A), then formulate the assignment decision as a covering optimization problem to minimize communication volume (Sec. V-B). We describe our solution algorithm (Sec. V-C). Finally, we analyze the theoretical benefits under different sparsity structures.

A. Workflow

Fig. 3 shows the workflow of five stages of our joint row-column communication strategy: ① **Matrix Sparsity Analysis:** Each process i analyzes the sparsity structure of its off-diagonal submatrices $\mathbf{A}^{(i,j)}$ to prepare for the subsequent optimization-based strategy selection. ② **Communication Strategy Selection:** Each process i solves a covering optimization problem to determine, for each nonzero in $\mathbf{A}^{(i,j)}$, whether to use row-based or column-based communication. Based on these decisions, $\mathbf{A}^{(i,j)}$ is partitioned into row-based and column-based components. Process i retains the column-based portion and transfers the row-based portion to remote process j . Note that steps ① and ② are performed offline as a preprocessing phase and can be reused across multiple SpMM operations with the same sparsity pattern. ③ **Remote Computation:** Process j computes partial \mathbf{C} results using the received row-based matrix portion and prepares required \mathbf{B} rows based on the column indices of process i ’s column-based portion. Both results are packed for transmission. ④ **Communication:** Process j transmits the computed partial \mathbf{C} results and required \mathbf{B} rows to process i . ⑤ **Result Aggregation:** Process i combines local computations with received \mathbf{B} rows and partial \mathbf{C} results to generate its final result $\mathbf{C}^{(i,:)}$.

B. Problem Formulation for Optimal Communication

As outlined in the workflow, the second stage involves solving an optimization problem to determine the optimal

communication strategy for each nonzero element. The key insight underlying this optimization is that each nonzero entry (i, j) in the off-diagonal submatrices of \mathbf{A} can be satisfied through either of two communication strategies: fetching the corresponding row of \mathbf{B} (column-based strategy using column index j) or computing and returning the corresponding row of \mathbf{C} (row-based strategy using row index i). Since multiple nonzero entries may share the same row or column indices, communication of a single row can satisfy multiple entries simultaneously. For example, as illustrated in Fig. 1(d), nonzero entries $\{b, c, d\}$ can be covered by communicating row $\mathbf{C}^{(0,:)}$ (row index 0), while entries $\{c, f, h\}$ can be covered by communicating row $\mathbf{B}^{(6,:)}$ (column index 6).

A naive solution to this problem would be to employ a greedy algorithm: count the number of nonzero entries covered by each row and column, sort them in descending order by coverage, and iteratively select rows or columns until all nonzero entries are covered. However, this greedy approach has two drawbacks: (1) it cannot guarantee global optimality, as greedy selections may lead to suboptimal overall communication costs, and (2) it incurs substantial overhead from iteratively counting coverage and updating statistics.

To address these limitations and achieve global optimality, we formalize the optimal strategy selection as a minimum weighted set cover problem, where the objective is to find the minimum-cost combination of \mathbf{B} -row and \mathbf{C} -row communications that covers all nonzero entries. Let $a_{ij} = 1$ if entry (i, j) in the off-diagonal submatrices of \mathbf{A} is nonzero, and $a_{ij} = 0$ otherwise. Since communicating rows of \mathbf{B} and \mathbf{C} may incur different costs due to varying data volumes and network paths, we introduce distinct cost coefficients and binary decision variables for each communication type. Specifically, for each column index j in the off-diagonal submatrices of \mathbf{A} (rows of \mathbf{B}):

$$x_j = \begin{cases} 1, & \text{if row } \mathbf{B}_{j,:} \text{ is communicated,} \\ 0, & \text{otherwise.} \end{cases} \quad (4)$$

with associated communication cost w_j^{col} . For each row index i in the off-diagonal submatrices of \mathbf{A} (rows of \mathbf{C}):

$$y_i = \begin{cases} 1, & \text{if row } \mathbf{C}_{i,:} \text{ is communicated,} \\ 0, & \text{otherwise,} \end{cases} \quad (5)$$

with associated communication cost w_i^{row} .

Optimization Model. The joint communication problem is formulated as:

$$\min \sum_j w_j^{\text{col}} x_j + \sum_i w_i^{\text{row}} y_i \quad (6)$$

$$\text{s.t. } x_j + y_i \geq a_{ij}, \quad \forall (i, j) \quad (7)$$

$$x_j, y_i \in \{0, 1\}, \quad \forall i, j \quad (8)$$

where constraint (7) ensures that each nonzero entry (i, j) in off-diagonal submatrices of \mathbf{A} is covered by communicating either row $\mathbf{B}_{j,:}$ (for column index) or row $\mathbf{C}_{i,:}$ (for row index).

C. Optimal Solution via Minimum Weighted Vertex Cover

1) *Formulation as a Graph Problem:* The optimization problem essentially concerns row-column relationships established through nonzero entries in sparse matrices. These relationships

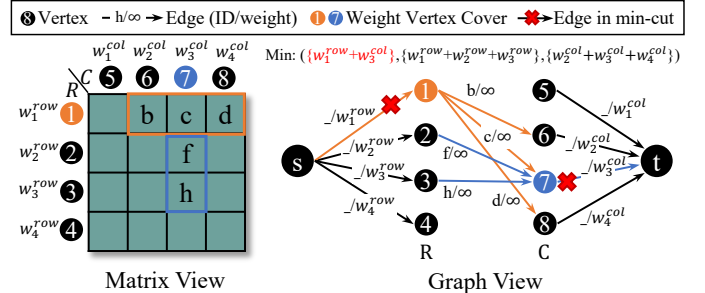


Fig. 4: Optimal communication volume via minimum weighted vertex cover. The matrix view (left) shows nonzero entries, while the graph view (right) models the problem as a flow network. Matrix nonzeros correspond to graph edges, while matrix rows and columns correspond to vertex sets \mathcal{R} and \mathcal{C} , respectively. The minimum s - t cut (red crosses) yields the optimal solution: communicate the row of \mathbf{C} indexed by row 1 and the row of \mathbf{B} indexed by column 7 to cover all nonzero entries b, c, d, f, h .

naturally map to bipartite graph structures where nonzeros correspond to edges. Therefore, we solve the weighted set cover problem by constructing a bipartite graph $G = (\mathcal{R} \cup \mathcal{C}, E)$ and transforming it into a minimum weighted vertex cover problem. Here, \mathcal{R} represents the set of row indices and \mathcal{C} represents the set of column indices from the off-diagonal submatrices of \mathbf{A} . The edge set $E = \{(i, j) \mid a_{ij} = 1, i \in \mathcal{R}, j \in \mathcal{C}\}$ connects row vertices to column vertices, with each edge $(i, j) \in E$ corresponding to a nonzero entry that requires communication coverage. The decision variables map directly to vertex selection: $y_i = 1$ means including row vertex $i \in \mathcal{R}$ in the vertex cover (communicating row $\mathbf{C}_{i,:}$), while $x_j = 1$ means including column vertex $j \in \mathcal{C}$ (communicating row $\mathbf{B}_{j,:}$). Each vertex is assigned a weight equal to its communication cost: w_i^{row} for row vertices and w_j^{col} for column vertices. This construction ensures that any vertex cover $U \subseteq \mathcal{R} \cup \mathcal{C}$ must include at least one endpoint of every edge, covering each nonzero entry (i, j) by either selecting row vertex i or column vertex j .

Thus, the minimum weighted set cover becomes the minimum weighted vertex cover problem on a bipartite graph, i.e., finding a minimum-weight vertex set covering all edges:

$$\min_{U \subseteq \mathcal{R} \cup \mathcal{C}} \sum_{i \in U \cap \mathcal{R}} w_i^{\text{row}} + \sum_{j \in U \cap \mathcal{C}} w_j^{\text{col}} \quad (9)$$

which directly corresponds to minimizing the total communication cost in our original formulation (Equation 6).

2) *Optimal Solution via Max-Flow Min-Cut:* To solve this vertex cover problem optimally, we further reduce it to a minimum s - t cut problem by constructing a flow network. This reduction exploits the well-established correspondence between minimum weighted vertex cover and minimum cut in bipartite graphs [34]–[36]. We build the flow network by adding source s and sink t , connecting s to each row vertex $i \in \mathcal{R}$ with capacity w_i^{row} , connecting each column vertex $j \in \mathcal{C}$ to t with capacity w_j^{col} , and assigning infinite capacity to all bipartite edges $(i, j) \in E$. Since the minimum s - t cut must

Pattern 1 (Row-skewed)	Pattern 2 (Col-skewed)	Pattern 3 (Uniform)	Pattern 4 (Mixed)
1 1 1 1	1 1	1	1 1 1 1
1 1 1 1	1 1	1	1
	1 1	1	1
	1 1	1	1
	Pattern 1	Pattern 2	Pattern 3
Rows(A)	2	4	4
Cols(A)	4	2	4
μ	2	2	4
Reduction(%)	0	0	50

Fig. 5: Different sparsity patterns and communication volume reduction.

avoid infinite-capacity edges, it can only cut finite-capacity edges, and the vertices corresponding to these cut edges form the optimal vertex cover.

Fig. 4 demonstrates this approach on an example matrix. The minimum cuts occur at $s \rightarrow 1$ and $7 \rightarrow t$, yielding the optimal vertex cover $\{1, 7\}$, which corresponds to communicating the row of \mathbf{C} indexed by row 1 and the row of \mathbf{B} indexed by column 7 to cover all nonzero entries. The max-flow min-cut theorem [37] guarantees that this solution achieves the minimum communication cost, since the cut value directly corresponds to the total communication volume in our original problem. This problem can be solved efficiently using the standard max-flow algorithm Dinic's algorithm [38], achieving $O(V^2E)$ time complexity where $V = |\mathcal{R}| + |\mathcal{C}|$ and E represents the number of edges in the flow network. Importantly, this optimization is performed offline: as long as the sparsity pattern of matrix \mathbf{A} remains unchanged, the computed communication strategy can be reused across multiple SpMM operations, effectively amortizing the overhead of solving the problem.

D. Theoretical Analysis of Communication Benefits

In this subsection, we analyze the theoretical performance benefits of our joint optimization approach compared to existing methods. Here, we consider the common case where the communication costs are uniform for \mathbf{B} rows and \mathbf{C} rows.

1) Dominance Analysis: For any off-diagonal submatrix $\mathbf{A}^{(j,i)}$, our joint optimization approach achieves communication volume

$$V_{\text{joint}}^{i,j} = \mu \cdot N \cdot sz_{dt} \quad (10)$$

where μ represents the size of the minimum vertex cover obtained from our bipartite graph optimization. We can quantify the relative communication reductions compared to baseline row-based and column-based strategies as

$$Red_{\text{col}} = 1 - \frac{\mu}{|\text{Cols}(\mathbf{A}^{(j,i)})|} \quad Red_{\text{row}} = 1 - \frac{\mu}{|\text{Rows}(\mathbf{A}^{(j,i)})|} \quad (11)$$

2) Communication Reduction by Sparsity Patterns: The minimum vertex cover size μ depends on how high-degree vertices distribute across row and column partitions in the bipartite graph. This distribution pattern determines the benefit.

Low-reduction scenarios occur when

$$\mu \approx \min \{|\text{Cols}(\mathbf{A}^{(j,i)})|, |\text{Rows}(\mathbf{A}^{(j,i)})|\} \quad (12)$$

Figure 5 illustrates two such cases: (1) skewed patterns where high-degree vertices cluster in one partition (Patterns 1-2), and

(2) uniform patterns where all vertices have similar low degrees (Pattern 3). Both cases require the vertex cover to include most vertices on one partition, limiting joint optimization benefits.

High-reduction scenarios occur when

$$\mu \ll \min \{|\text{Cols}(\mathbf{A}^{(j,i)})|, |\text{Rows}(\mathbf{A}^{(j,i)})|\} \quad (13)$$

This requires high-degree vertices distributed across both partitions, enabling efficient bipartite coverage. Pattern 4 in Figure 5 demonstrates this: high-degree vertices on both sides create complementary coverage, achieving 50% reduction compared to single-strategy approaches where only one partition is utilized.

In summary, the reduction potential is determined by the sparsity pattern characteristics. When high-degree vertices are well-distributed across both partitions, the joint strategy achieves significant communication savings; conversely, skewed or uniform patterns limit the optimization gains. Nonetheless, the joint strategy guarantees no performance degradation as it generalizes both single strategies as special cases.

VI. HIERARCHICAL COMMUNICATION STRATEGY

This section presents how we adapt the joint row-column communication strategy to hierarchical networks. As discussed in Sec. III, flat communication patterns create redundant inter-group transfers. To address this, we separate the joint strategy into *row-based* and *column-based* communication, partition them into *fine-grained stages* to eliminate inter-group redundancy (Sec. VI-A), and recombine them through *complementary scheduling* to fully utilize the bandwidth of different tier links (Sec. VI-B).

A. Inter-group Redundancy Elimination

1) Communication Pattern Separation: The joint optimization result combines *row-based* and *column-based* communications. However, these exhibit different redundancy patterns in hierarchical networks. Specifically, *column-based* communication shows multiple processes fetching the same \mathbf{B} rows across group boundaries (e.g., B_0, B_1, B_2 transmitted multiple times from Group0 to Group1 in Figure 6(b)), while *row-based* communication has processes independently sending partial results that could be pre-aggregated (e.g., $C00, C10, C30$ rows sent separately in Figure 6(c)). These distinct redundancy patterns motivate our approach: we separate the joint communication plan into *row-based* and *column-based* operations, enabling targeted optimization for each pattern.

2) Hierarchical Aggregation Strategies: We eliminate inter-group redundancy through hierarchical-aware aggregation strategies specific to *row-based* and *column-based* communication respectively:

Column-based redundancy elimination. For matrix \mathbf{B} distribution, we adopt a three-step method [28]: (1) source group aggregation, (2) inter-group transfer, and (3) intra-group distribution. Specifically, process P_3 in Group0 first collects all its \mathbf{B} rows required by Group1 processes (P_4-P_7), obtaining the deduplicated set $\{B_0, B_1, B_2, B_3\}$ (Step 1). It then performs a single *inter-group* transfer (Step 2, i.e. Fig. 6(d) Stage 1) to Group1's representative, which distributes the rows internally

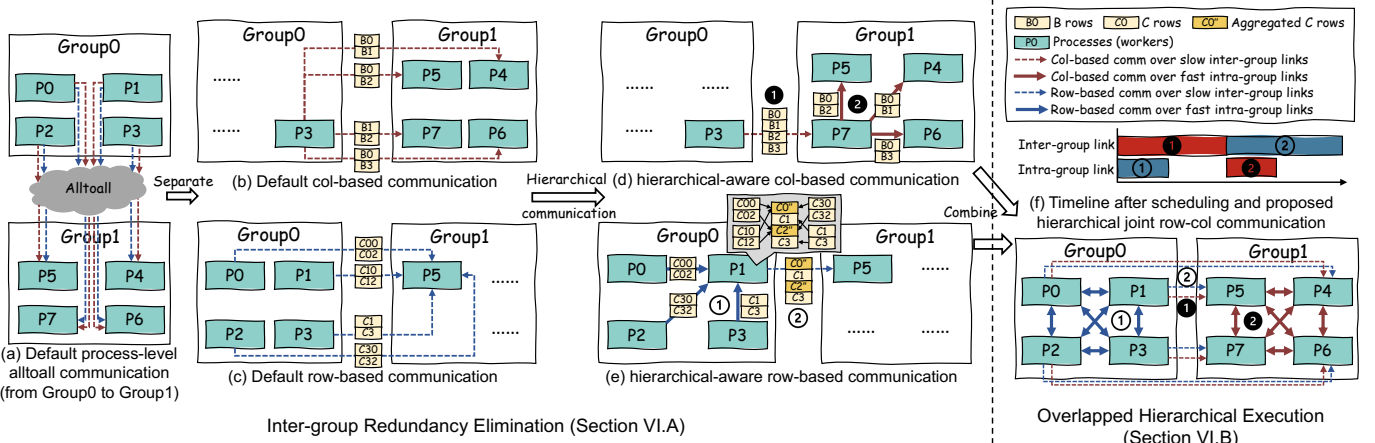


Fig. 6: Overview of hierarchical communication strategy. For clarity, only Group0-to-Group1 transfers are shown (reverse direction omitted), and row/column-based communication illustrates operations for a single process (others operate similarly).

using fast *intra-group* links (Step 3, i.e. Fig. 6(d) Stage ②). This reduces inter-group traffic from 8 to 4 row transfers, ensuring each unique row crosses group boundaries only once.

Row-based redundancy elimination. For matrix \mathbf{C} partial results, we propose a two-stage hierarchical aggregation: (1) *intra-group* pre-aggregation of partial results, and (2) *inter-group* transmission of aggregated data. In the first stage, a representative process within each source group collects partial \mathbf{C} results from group members and aggregates those destined for the same final \mathbf{C} rows (Fig. 6(e) stage ①). Figure 6(e) shows process P_1 in Group0 collects partial results from P_0 , P_2 , and P_3 , then sums partial results targeting the same output \mathbf{C} row (e.g., aggregating C_{00} , C_{10} , C_{30} into C''_0). This pre-aggregation uses fast *intra-group* links and reduces the data volume before crossing group boundaries. In the second stage, the representative transmits only the aggregated results to target processes in Group1 (Fig. 6(e) stage ②). This approach reduces *inter-group* transfers from 8 partial results to 4 aggregated results, decreasing traffic over slow inter-group links.

B. Overlapping Complementary Stages

In this section, we design an overlapping scheduling strategy for row- and column-based communication (Sec. VI-B1) and present its implementation workflow (Sec. VI-B2).

1) *Scheduling Complementary Stages:* The row-based and column-based redundancy elimination (Sec. VI-A2) exhibit natural complementarity: when one uses intra-group links, the other uses inter-group links. This complementary execution order is determined by the source of redundancy in each type. Row-based communication must aggregate partial results within source groups before inter-group transmission (Fig. 6(e) ①→②), while column-based communication must fetch data across groups before intra-group distribution in destination groups (Fig. 6(d) ①→②).

Since no dependencies exist between row- and column-based communications, we exploit this complementary network usage through a two-stage overlapping strategy (Fig. 6(f)). Stage I pairs row-based intra-group aggregation (Fig. 6(f) ①) with column-based inter-group fetching (Fig. 6(f) ①), allowing source groups to aggregate partial results with intra-group

Algorithm 1: Hierarchical Group Communication for Distributed SpMM (per-process view)

Input: Local sparse matrix blocks \mathbf{A}_{row} , \mathbf{A}_{col} ; Dense matrix \mathbf{B} ; Group ID g_{id}
Output: B_{dist} (column-based communication result), C_{recv} (row-based communication result)

```

1 I.①: Inter-group B fetch (Column-based)
2 for each group  $g \neq g_{id}$  do
3    $B_{send}^g \leftarrow \text{CollectRequiredRows}(g, \mathbf{A}_{col}, \mathbf{B})$ 
4   InterGroupSendRecv( $B_{send}^g$ ,  $B_{recv}^g$ ,  $g$ ) ▷ Non-blocking
5 I.②: Intra-group C aggregation (Row-based)
6  $C_{row} \leftarrow \text{SpMM}(\mathbf{A}_{row}, \mathbf{B})$ 
7 IntraGroupAlltoall( $C_{row}$ ,  $C_{partial}$ )
8 II.②: Inter-group C transmission (Row-based)
9 for each group  $g \neq g_{id}$  do
10    $C_{agg}^g \leftarrow \text{Aggregate}(C_{partial}, g)$ 
11   InterGroupSendRecv( $C_{agg}^g$ ,  $C_{recv}^g$ ,  $g$ ) ▷ Non-blocking
12 II.②: Intra-group B distribution (Column-based)
13 WaitRecv( $B_{recv}$ )
14 IntraGroupAlltoall( $B_{recv}$ ,  $B_{dist}$ )
15 WaitRecv( $C_{recv}$ )
16 return  $B_{dist}$ ,  $C_{recv}$ 
▷ Wait for Stage I.①
▷ Wait for Stage II.②

```

links while destination groups simultaneously fetch required data with inter-group links. Stage II reverses this pattern: row-based inter-group transmission (Fig. 6(f) ②) occurs alongside column-based intra-group distribution (Fig. 6(f) ②), ensuring aggregated results cross group boundaries while fetched data is distributed within destination groups. This complementary execution maintains continuous utilization of both network tiers without contention.

2) *Communication Workflow:* Fig. 6(f) and Alg. 1 present the complete hierarchical communication from a per-process perspective. The algorithm takes local sparse matrix blocks \mathbf{A}_{row} and \mathbf{A}_{col} , dense matrix \mathbf{B} , and group ID as inputs, executing two stages of parallel row-column communications. Stage I combines column-based inter-group B fetching (lines 1-4, stage I.①), where processes collect and send required B rows to peers in other groups, with row-based intra-group C aggregation (lines 5-7, stage I.②), where processes compute SpMM with \mathbf{A}_{row} then exchange partial C results within groups. Stage II then pairs row-based inter-group C transmission (lines 8-

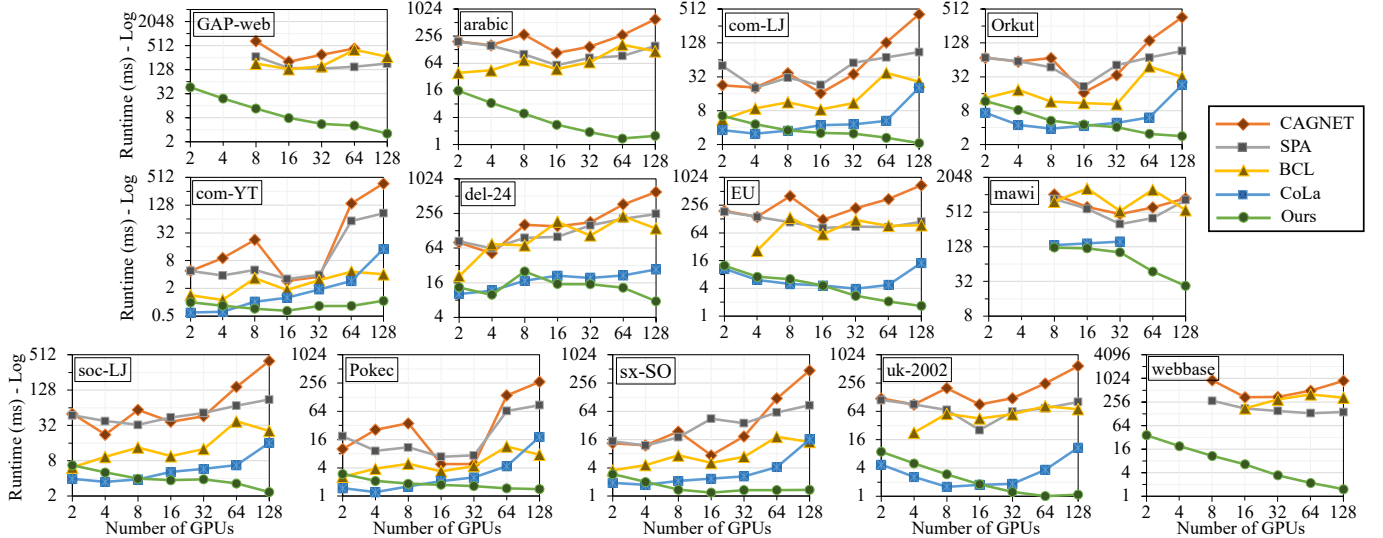


Fig. 7: Runtime comparison (Y-axis log-scale) with baselines and strong scaling for different datasets. Due to out-of-memory (OOM) and runtime errors, some data could not be collected. The dense columns number (N) is 32.

TABLE II: Sparse Matrices Datasets

Matrix	#rows/cols	#nonzeros	Density
com-Youtube (com-YT)	1.1M	6.0M	4.64e-06
soc-Pokec (Pokec)	1.6M	30.6M	1.15e-05
sx-stackoverflow (sx-SO)	2.6M	36.2M	5.35e-06
soc-LiveJournal (soc-LJ)	4.8M	69.0M	2.94e-06
com-LiveJournal (com-LJ)	4.0M	69.4M	4.34e-06
delaunay_n24 (del24)	16.8M	100.7M	3.58e-07
europe_osm (EU)	50.9M	108.1M	4.17e-08
mawi_69M (mawi)	68.9M	143.4M	3.02e-08
com-Orkut (Orkut)	3.1M	234.4M	2.48e-05
uk-2002 (uk-2002)	18.5M	298.1M	8.69e-07
arabic-2005 (arabic)	22.7M	640.0M	1.24e-06
webbase-2001 (webbase)	118.1M	1.02B	7.31e-08
GAP-web (GAP-web)	50.6M	1.93B	7.53e-07

11, stage II.②), where processes aggregate the partial results from stage I.① destined for the same remote peer before transmission, with column-based intra-group B distribution (lines 12-14, stage II.②), where processes redistribute the B rows received in stage I.① within their groups. The algorithm synchronizes both communication stages (lines 13 and 15) and returns the received results: B_{dist} from column-based communication and C_{recv} from row-based communication, which can be used for further computations.

VII. EVALUATION

A. Experimental Setup

1) *Hardware*: All experiments are conducted on the TSUB-AME4.0 supercomputer [31]. Each compute node is equipped with dual AMD EPYC 9654 processors and 4 Nvidia H100 SXM5 GPUs with 94GB HBM2e memory, interconnected via NVLink 4.0 providing 450GB/s unidirectional link bandwidth per GPU. The nodes are interconnected via InfiniBand NDR200 with 200Gbps bandwidth in a fat-tree topology.

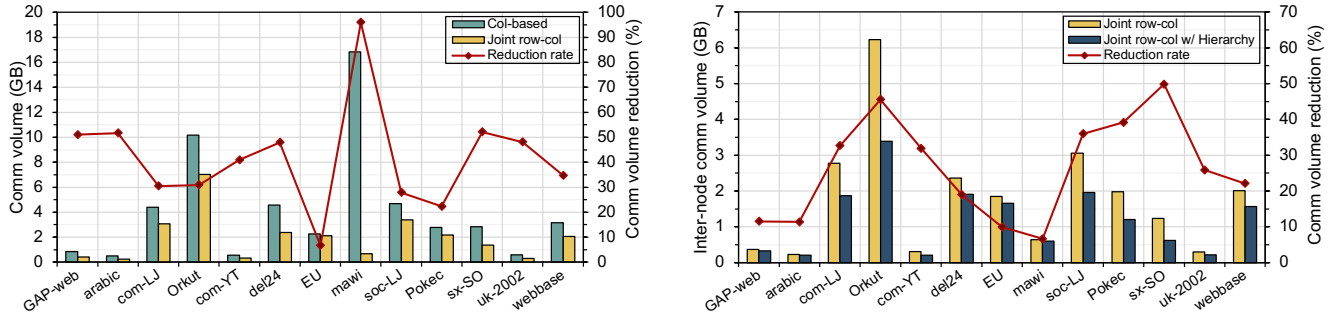
2) *Datasets*: We use diverse sparse matrices from the SuiteSparse Matrix Collection [39] (Tab. II) that span multiple domains with varying sparsity patterns, and are widely used in recent related work [22], [24], [28].

3) *Implementation*: For single-node SpMM, we use PyTorch (v2.5.1)'s `torch.sparse.mm` [40], which calls CSR version's SpMM in cuSPARSE [41]. Multi-node communication is implemented using PyTorch distributed [42] with NCCL (v2.21.5) backend [43], utilizing `alltoall` primitive.

4) *Baselines*: To validate the effectiveness of our methods, we select baselines sharing similar design choices with our approach except for key differences in: (1) matrix partitioning (1D, 1.5D, 2D); (2) sparsity awareness (oblivious vs. aware); and (3) hierarchy awareness (oblivious vs. aware). Specifically, we compare against four state-of-the-art distributed SpMM methods: CAGNET [25] (1.5D/stationary A, sparsity-oblivious, NCCL [43]), SPA [26] (1.5D/stationary A, column-based sparsity-aware, NCCL [43]), BCL [2] (2D/stationary C, sparsity-oblivious, NVSHMEM [44]), and CoLa [28] (1D/stationary A, column-based sparsity-aware with hierarchical-awareness, NVSHMEM [44]). For CAGNET and SPA, we extract the core SpMM component from their GNN implementations and set the replication factor to 4, which delivers near-optimal performance in their original papers. Matrix (graph) reordering is disabled to ensure fair comparison and maintain applicability to diverse matrix types. We conduct 5 warm-up runs followed by 100 timed runs. We collect the end-to-end execution time of each run and report the average time over the 100 runs.

B. Overall Performance

In this subsection, we compare our method with baselines across different datasets and GPU counts with 32 dense columns, as shown in Figure 7. Some results are omitted due to out-of-memory (OOM) or runtime errors. Compared to BCL and CAGNET, which need to fetch B blocks (CAGNET) or both A and B blocks (BCL) without considering sparsity patterns, our method consistently outperforms them across all GPU counts and datasets. Notably, CAGNET's poor performance stems from decomposing collective communication into multiple synchronous broadcasts, causing process idling and low network utilization. These results demonstrate the



(a) Comparison of total global communication volume between the default Col-based strategy and joint row-col strategy.
(b) Comparison of total inter-node communication volume between joint row-column strategy and the same strategy with hierarchical communication.
Fig. 8: Global communication volume reduction by joint row-col based communication and inter-node communication volume reduction by hierarchical communication strategy. nGPUs = 32, $N = 64$.

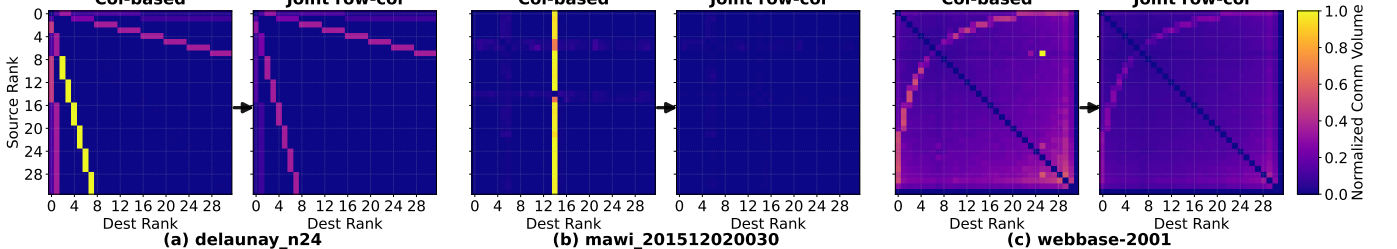


Fig. 9: Inter-process communication patterns before and after applying joint row-column strategy across datasets: achieving lower volume and better balance. Communication volumes are normalized by the maximum value within each respective dataset.
benefit of sparsity-aware communication strategies on diverse sparsity patterns. Additionally, our method also outperforms SPA, which employs col-based communication but lacks our joint row-column and hierarchical optimizations.

Compared to CoLa, our method is slower when using 4 or fewer GPUs because each TSUBAME node contains 4 GPUs interconnected with all-to-all NVLink. At this scale, intra-node communication overhead is minimal and computation remains the bottleneck, where CoLa’s computational optimizations and fine-grained RDMA communication for better computation-communication overlap provide better performance. However, when scaling to 8 or more GPUs across multiple nodes, communication becomes the primary bottleneck and our method outperforms CoLa on most datasets, with speedups increasing as GPU count grows. This confirms that our communication optimizations effectively reduce communication overhead and improve overall SpMM performance at scale.

C. Scaling

Figure 7 demonstrates the strong scaling of our method compared to baselines across different datasets. The experiment starts from 2 GPUs to 128 GPUs. All baselines can only scale up to 8 GPUs (2 compute nodes), after which execution time increases with additional GPUs due to communication overhead. In contrast, our method exhibits decreasing execution time as GPU count grows on most datasets, scaling up to 128 H100 GPUs. Notably, our method achieves high scaling efficiency on datasets such as GAP-web, uk-2002, and webbase. This strong scaling result further validates that our method effectively reduces communication overhead, which is the primary impediment to scalability.

D. Effectiveness of proposed methods

1) *Reduction in Communication Volumes*: We conduct experiments on 32 GPUs with 64 dense columns.

Joint row-column sparsity-aware strategy. We compare the total communication volume between the default column-based strategy and our joint row-column strategy. Figure 8(a) shows the total communication volume and the reduction ratio achieved by our method. The reduction ratio varies across different datasets, but our method consistently reduces communication volume on all datasets, validating its effectiveness for communication optimization. Notably, our method achieves the most significant reduction on the mawi dataset, eliminating 96% of the communication volume compared to the default strategy. This communication reduction translates directly to performance gains, as mawi also exhibits the highest speedup (nearly 6 \times) in the overall runtime results presented later.

We also analyze the inter-process communication patterns between column-based and joint row-column communication strategies, as illustrated in Fig. 9. Due to space limitations, we present three representative datasets that exhibit more imbalanced communication patterns compared to others. In these heatmaps, the y-axis represents the source rank and the x-axis represents the destination rank, with brighter regions indicating higher communication volume between rank pairs. Across all three datasets, the joint row-column strategy not only reduces the overall communication volume but also significantly diminishes the communication between previously heavy-communicating rank pairs (eliminating the bright spots in the figures), resulting in a more balanced communication pattern. Notably, two of these datasets (delaunay_n24 and mawi) correspond to symmetric matrices from undirected

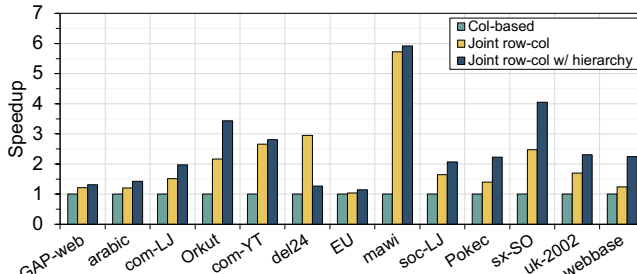


Fig. 10: Step-wise optimization (runtime) results. nGPUs = 32, $N = 64$.

graphs, where the ideal communication pattern should also be symmetric. While the column-based strategy produces asymmetric and imbalanced patterns, our joint row-column strategy preserves the inherent symmetry of the communication. A more balanced communication pattern typically translates to better performance for all-to-all communication.

Hierarchical communication strategy. Building on our joint row-column strategy, we compare the total inter-node communication volume with and without the hierarchical communication strategy, as shown in Figure 8(b). Similarly, the reduction varies across matrices, but our hierarchical strategy consistently reduces inter-node communication on all datasets. The reduction is particularly pronounced on com-LJ, Orkut, Pokec, and sx-SO datasets, which correspondingly demonstrate substantial improvements in the overall runtime results.

2) *Reduction in Overall Runtime:* Figure 10 presents ablation study results with 64 dense columns on 32 GPUs. The relative speedups of both methods vary across datasets, reflecting the diverse communication patterns inherent to different sparse matrix structures. Specifically, our joint row-column communication strategy consistently achieves speedups across all datasets, demonstrating its ability to reduce communication redundancy and improve overall performance. The hierarchical communication strategy delivers performance gains on most datasets, demonstrating that our approach reduces inter-group communication while maintaining high network link utilization, thereby improving both communication and overall performance. The only exception is del24, which exhibits highly imbalanced communication patterns. For this case, decomposing a collective communication into smaller hierarchical communications reduces network link utilization, thereby degrading performance. Overall, the runtime results validate our communication analysis: datasets with greater communication reduction consistently achieve higher speedups across both optimization methods.

E. Performance of Different Numbers of Dense Columns

To assess the sensitivity of our approach to the number of dense columns (N), we evaluate its performance under different N values: 32, 64, and 128, as shown in Figure 11. On most datasets, our method exhibits linear scaling with N , indicating that the execution is communication throughput-bound. However, on datasets such as arabic, the execution becomes communication latency-bound rather than throughput-

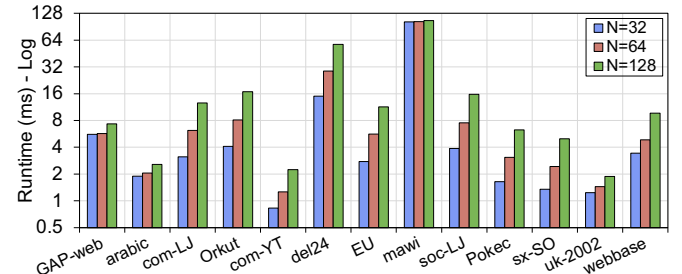


Fig. 11: Performance of different numbers of dense columns $N = \{32, 64, 128\}$. nGPUs = 32.

bound, as the reduced data volume shifts the bottleneck from bandwidth to latency.

VIII. RELATED WORK

A. Distributed SpMM

Much prior work on distributed SpMM has focused on communication-avoiding strategies, including 1D and 2D partitionings with replication [21]. Later work focused on various algorithms for tall-skinny dense matrix multiplication [27], as is common for GNN and other machine learning applications, as well as asynchronous RDMA-based algorithms to avoid load imbalance issues [2]. Communication-avoiding techniques have been applied to GNNs and other domains [25], [29], yet primarily use sparsity-oblivious methods and exploit sparsity structure only through traditional matrix permutation.

Recent work has explored sparsity-aware communication strategies for distributed SpMM. Several methods [23], [26], [28] proposed sparsity-aware approaches that primarily employ column-based strategies. Abubaker et al. [24] introduced a hybrid approach that combines both row-based and column-based sparsity-aware strategies. However, these methods consider row-based and column-based strategies separately, leading to communication redundancy. Another direction explored by [22] is adaptively choosing between P2P and collective communication for different matrix blocks based on sparsity patterns, which is orthogonal to our approach. Other work has explored using sparsity-aware techniques (column-based strategy) to optimize sparse-sparse matrix multiplication (SpGEMM) [45].

Another line of research reduces communication overhead through graph partitioning or matrix decomposition techniques. For example, prior work reduces communication through arrow matrix decomposition [46] or hypergraph partitioning [23]. These methods optimize communication patterns through matrix partitioning. Our method operates at a different level: it optimizes the communication strategy for patterns produced by any partitioning algorithm. This orthogonality allows our approach to be directly applied on top of these partitioning schemes for additional communication overhead reduction.

B. Distributed GNN

Several works have focused on optimizing distributed GNN training, where SpMM-like operations constitute the primary performance bottleneck. The most closely related work [47] also reduces communication overhead in GNN training through similar strategies, but is tailored to graph-structured data and

does not consider hierarchical networks. Other works, such as [25], [26], [29], [30], accelerated distributed GNN training through different approaches to reduce SpMM communication overhead. Some works [47]–[49] used lossy compression to reduce GNN training communication, but such methods are inapplicable to scientific SpMM requiring exact results.

IX. CONCLUSION

In this paper, we propose a communication-efficient distributed framework, SHIRO, to address the communication bottleneck in distributed sparse matrix-matrix multiplication (SpMM). We address inefficient communication strategies by: (1) a fine-grained, sparsity-aware communication strategy that exploits sparsity patterns to eliminate redundant data transfers, and (2) a hierarchical communication strategy that leverages two-tier network architectures to minimize communication across slow network links. Extensive experiments on real-world datasets demonstrate that our approach reduces communication overhead effectively and improves performance significantly.

REFERENCES

- [1] A. Tiskin, “All-pairs shortest paths computation in the bsp model,” in *International Colloquium on Automata, Languages, and Programming*. Springer, 2001, pp. 178–189.
- [2] B. Brock, A. Buluç, and K. Yelick, “Rdma-based algorithms for sparse matrix multiplication on gpus,” in *Proceedings of the 38th ACM International Conference on Supercomputing*, 2024, pp. 225–235.
- [3] D. P. O’Leary, “The block conjugate gradient algorithm and related methods,” *Linear algebra and its applications*, vol. 29, pp. 293–322, 1980.
- [4] R. G. Grimes, J. G. Lewis, and H. D. Simon, “A shifted block lanczos algorithm for solving sparse symmetric generalized eigenproblems,” *SIAM Journal on Matrix Analysis and Applications*, vol. 15, no. 1, pp. 228–272, 1994.
- [5] M. Sadkane, “A block arnoldi-chebyshev method for computing the leading eigenpairs of large sparse unsymmetric matrices,” *Numerische mathematik*, vol. 64, no. 1, pp. 181–193, 1993.
- [6] M. H. Gutknecht, “Block krylov space methods for linear systems with multiple right-hand sides: an introduction,” in *Modern mathematical models, methods and algorithms for real world systems*. Anshan, 2007, pp. 420–447.
- [7] J. Gilmer, S. S. Schoenholz, P. F. Riley, O. Vinyals, and G. E. Dahl, “Neural message passing for quantum chemistry,” in *Proceedings of the 34th International Conference on Machine Learning*, ser. Proceedings of Machine Learning Research, D. Precup and Y. W. Teh, Eds., vol. 70. PMLR, 2017, pp. 1263–1272.
- [8] M. Fey and J. E. Lenssen, “Fast graph representation learning with PyTorch Geometric,” *arXiv preprint arXiv:1903.02428*, 2019, iCLR Workshop on Representation Learning on Graphs and Manifolds.
- [9] M. Wang, D. Zheng, Z. Ye, Q. Gan, M. Li, X. Song, J. Zhou, C. Ma, L. Yu, Y. Gai, T. Xiao, T. He, G. Karypis, J. Li, and Z. Zhang, “Deep graph library: A graph-centric, highly-performant package for graph neural networks,” *arXiv preprint arXiv:1909.01315*, 2019.
- [10] X. He, L. Liao, H. Zhang, L. Nie, X. Hu, and T.-S. Chua, “Neural collaborative filtering,” in *Proceedings of the 26th International Conference on World Wide Web*. International World Wide Web Conferences Steering Committee, 2017, pp. 173–182.
- [11] Q. Wang, Z. Mao, B. Wang, and L. Guo, “Knowledge graph embedding: A survey of approaches and applications,” *IEEE Transactions on Knowledge and Data Engineering*, vol. 29, no. 12, pp. 2724–2743, 2017.
- [12] T. Gale, M. Zaharia, C. Young, and E. Elsen, “Sparse gpu kernels for deep learning,” in *SC20: International Conference for High Performance Computing, Networking, Storage and Analysis*. IEEE, 2020, pp. 1–14.
- [13] Z. Ye, R. Lai, J. Shao, T. Chen, and L. Ceze, “Sparsetir: Composable abstractions for sparse compilation in deep learning,” in *Proceedings of the 28th ACM International Conference on Architectural Support for Programming Languages and Operating Systems, Volume 3*, 2023, pp. 660–678.
- [14] R. Fan, W. Wang, and X. Chu, “Dtc-spmm: Bridging the gap in accelerating general sparse matrix multiplication with tensor cores,” in *Proceedings of the 29th ACM International Conference on Architectural Support for Programming Languages and Operating Systems, Volume 3*, 2024, pp. 253–267.
- [15] Y. Wang, B. Feng, Z. Wang, G. Huang, and Y. Ding, “{TC-GNN}: Bridging sparse {GNN} computation and dense tensor cores on {GPUs},” in *2023 USENIX Annual Technical Conference (USENIX ATC 23)*, 2023, pp. 149–164.
- [16] M. Pang, X. Fei, P. Qu, Y. Zhang, and Z. Li, “A row decomposition-based approach for sparse matrix multiplication on gpus,” in *Proceedings of the 29th ACM SIGPLAN Annual Symposium on Principles and Practice of Parallel Programming*, 2024, pp. 377–389.
- [17] O. Schenk and K. Gärtnner, “Solving unsymmetric sparse systems of linear equations with pardiso,” *Future Generation Computer Systems*, vol. 20, no. 3, pp. 475–487, 2004.
- [18] W. Hu, M. Fey, M. Zitnik, Y. Dong, H. Ren, B. Liu, M. Catasta, and J. Leskovec, “Open graph benchmark: Datasets for machine learning on graphs,” *arXiv preprint arXiv:2005.00687*, 2020.
- [19] J. Leskovec and A. Krevl, “SNAP Datasets: Stanford large network dataset collection,” <http://snap.stanford.edu/data>, June 2014.
- [20] J. Leskovec and R. Sosić, “Snap: A general-purpose network analysis and graph-mining library,” *ACM Transactions on Intelligent Systems and Technology*, vol. 8, no. 1, pp. 1–20, 2016.
- [21] P. Koanantakool, A. Azad, A. Buluç, D. Morozov, S.-Y. Oh, L. Oliker, and K. Yelick, “Communication-avoiding parallel sparse-dense matrix-matrix multiplication,” in *2016 IEEE International Parallel and Distributed Processing Symposium (IPDPS)*. IEEE, 2016, pp. 842–853.
- [22] C. Block, G. Gerogiannis, C. Mendis, A. Azad, and J. Torrellas, “Two-face: Combining collective and one-sided communication for efficient distributed spmm,” in *Proceedings of the 29th ACM International Conference on Architectural Support for Programming Languages and Operating Systems, Volume 2*, 2024, pp. 1200–1217.
- [23] S. Acer, O. Selvitopi, and C. Aykanat, “Improving performance of sparse matrix dense matrix multiplication on large-scale parallel systems,” *Parallel Computing*, vol. 59, pp. 71–96, 2016.
- [24] N. Abubaker and T. Hoefler, “Spcomm3d: A framework for enabling sparse communication in 3d sparse kernels,” *arXiv preprint arXiv:2404.19638*, 2024.
- [25] A. Tripathy, K. Yelick, and A. Buluç, “Reducing communication in graph neural network training,” in *SC20: International Conference for High Performance Computing, Networking, Storage and Analysis*. IEEE, 2020, pp. 1–14.
- [26] U. Mukhopadhyay, A. Tripathy, O. Selvitopi, K. Yelick, and A. Buluç, “Sparsity-aware communication for distributed graph neural network training,” in *Proceedings of the 53rd International Conference on Parallel Processing*, 2024, pp. 117–126.
- [27] O. Selvitopi, B. Brock, I. Nisa, A. Tripathy, K. Yelick, and A. Buluç, “Distributed-memory parallel algorithms for sparse times tall-skinny-dense matrix multiplication,” in *Proceedings of the 35th ACM International Conference on Supercomputing*, 2021, pp. 431–442.
- [28] L. Zhang, Y. Shao, and S. Li, “Cola: Towards communication-efficient distributed sparse matrix-matrix multiplication on gpus,” in *Proceedings of the 39th ACM International Conference on Supercomputing*, 2025, pp. 73–87.
- [29] V. Bharadwaj, A. Buluç, and J. Demmel, “Distributed-memory sparse kernels for machine learning,” in *2022 IEEE International Parallel and Distributed Processing Symposium (IPDPS)*. IEEE, 2022, pp. 47–58.
- [30] M. F. Balin, K. Sancak, and U. V. Catalyurek, “Mg-gcn: a scalable multi-gpu gcn training framework,” in *Proceedings of the 51st International Conference on Parallel Processing*, 2022, pp. 1–11.
- [31] Institute of Science Tokyo, “Tsubame4.0 user’s guide,” <https://www.t4.cii.iict.ac.jp/docs/handbook.en/>, 2024.
- [32] NVIDIA Corporation, “NVIDIA H100 Tensor Core GPU,” <https://www.nvidia.com/en-us/data-center/h100/>, 2024, accessed: 2024.
- [33] Mellanox Technologies, “Introducing 200G HDR InfiniBand Solutions,” <https://network.nvidia.com/files/doc-2020/wp-introducing-200g-hdr-infiniband-solutions.pdf>, 2019, accessed: 2024.
- [34] D. König, “Graphok és matrixok,” *Matematikai és Fizikai Lapok*, vol. 38, pp. 116–119, 1931.
- [35] A. Schrijver, *Combinatorial optimization: polyhedra and efficiency*. Springer Science & Business Media, 2003, vol. 24.
- [36] J. Egerváry, “Matrixok kombinatorius tulajdonságairól,” *Matematikai és Fizikai Lapok*, vol. 38, no. 1931, pp. 16–28, 1931.

- [37] L. R. Ford Jr and D. R. Fulkerson, “Maximal flow through a network,” *Canadian Journal of Mathematics*, vol. 8, pp. 399–404, 1956.
- [38] E. A. Dinic, “Algorithm for solution of a problem of maximum flow in networks with power estimation,” *Soviet Mathematics Doklady*, vol. 11, pp. 1277–1280, 1970.
- [39] T. A. Davis and Y. Hu, “The university of florida sparse matrix collection,” *ACM Transactions on Mathematical Software*, vol. 38, no. 1, pp. 1–25, 2011.
- [40] A. Paszke, S. Gross, F. Massa *et al.*, “Pytorch: An imperative style, high-performance deep learning library,” *Advances in Neural Information Processing Systems*, vol. 32, 2019.
- [41] NVIDIA Corporation, “cusparse library,” <https://developer.nvidia.com/cusparse>, 2024.
- [42] PyTorch Team, “Pytorch distributed,” <https://docs.pytorch.org/docs/stable/distributed.html>, 2024.
- [43] NVIDIA Corporation, “Nccl: Nvidia collective communication library,” <https://developer.nvidia.com/nccl>, 2024.
- [44] ———, “Nvshmem,” <https://developer.nvidia.com/nvshmem>, 2024.
- [45] Y. Hong and A. Buluç, “A sparsity-aware distributed-memory algorithm for sparse-sparse matrix multiplication,” in *Proceedings of the International Conference for High Performance Computing, Networking, Storage, and Analysis*, ser. SC ’24. IEEE Press, 2024. [Online]. Available: <https://doi.org/10.1109/SC41406.2024.00053>
- [46] L. Gianinazzi, A. N. Ziogas, L. Huang, P. Luczynski, S. Ashkboosh, F. Scheidl, A. Carigiet, C. Ge, N. Abubaker, M. Besta *et al.*, “Arrow matrix decomposition: A novel approach for communication-efficient sparse matrix multiplication,” in *Proceedings of the 29th ACM SIGPLAN Annual Symposium on Principles and Practice of Parallel Programming*, 2024, pp. 404–416.
- [47] C. Zhuang, L. Zhang, D. Wu, P. Chen, J. Huang, X. Liu, R. Yokota, N. Dryden, T. Endo, S. Matsuoka *et al.*, “Scaling large-scale gnn training to thousands of processors on cpu-based supercomputers,” in *Proceedings of the 39th ACM International Conference on Supercomputing*, 2025, pp. 57–72.
- [48] C. Wan, Y. Li, A. Li, N. S. Kim, and Y. Lin, “Bns-gen: Efficient full-graph training of graph convolutional networks with partition-parallelism and random boundary node sampling,” *Proceedings of Machine Learning and Systems*, vol. 4, pp. 673–693, 2022.
- [49] B. Wan, J. Zhao, and C. Wu, “Adaptive message quantization and parallelization for distributed full-graph gnn training,” *Proceedings of Machine Learning and Systems*, vol. 5, pp. 203–218, 2023.